

Influence of Top Layer's Material and Flow Direction on Mass Transfer through Multi-Layer Ceramic Membranes for Membrane Reactors

Arshad Hussain*, A. Seidel-Morgenstern**, E. Tsotsas**

*School of Chemical and Materials Engineering,
National University of Science & Technology, Islamabad, Pakistan
arshad-ccems@nust.edu.pk

Max-Planck-Institut für Dynamik komplexer technischer Systeme
**Institute of Process Engineering, Otto-von-Guericke-University Magdeburg, Germany

Abstract

The influence of top layer's material of membrane and flow direction on gas transport has been investigated. A simulation analysis has been done to study the influence of the material of permselective layer (top membrane layer) temperature and the direction of gas flow on the mass transfer through a composite membrane. Dusty gas model for single gas permeation has been used to study these effects. It is obvious from analysis that apart from top layer's material, flow direction has also an influence on the mass transfer through composite membrane.

Keywords: Gas Permeation, Permselective Layer, Mass Transfer, Dusty Gas Model, Membrane Reactor

Introduction

The influence of composite nature of the membrane on the gas transport has been investigated, though mostly focused on polymeric composite membranes [1-3], to explain the membrane performance and selectivity. The asymmetry of the membrane can be used to facilitate the diffusion of one of the reactants while hindering the other one. Successive layers of different thicknesses and materials can also contribute to carrying out different consecutive reactions in different regions of the membrane [4]. The permeability of the membrane may also not be uniform along the entire length. The formation of top layer of different thickness on the support layer is a complicated process, which demands a perfect interaction between the materials of top and intermediate/support layers to produce a good composite membrane. But in practice it has been found that the structure of top layer is far from being homogenous throughout its thickness. Some regions adjoining the top layer to the support/intermediate layer can be abrupted. This shortcoming can be attributed to the phenomena of deformation-orientational order that occur during the formation of selective, thin layer on a porous support [5]. Hence, the nature of material and interaction between the material of top layer and the support profoundly affects the structure and properties of the composite membrane [6]. It has also been revealed from a simulation analysis that the direction of gas flow has also an influence on the mass transfer through composite membrane

Membrane characterization

Much effort has been devoted to the problem of predicting the parameters of a porous membrane. Dusty Gas Model (DGM) [7-9] is widely used to characterize the porous membranes. From the practical point of view, it is still better to determine these parameters directly by mass transfer experiments. To test a theory whose mathematical formulation is based on adjustable parameters, a comprehensive set of experiments is required to determine

the model parameters. Mass transfer experiments enable the identification and validation of all mass transport parameters of the membrane. Single gas permeation experiments (Fig. 1) have been performed mainly for the identification of structural parameters of every membrane layer by using air, N₂ and He for different temperatures (20-500 °C) and pressures (1-3 bar).

Single gas permeation experiments

The principle of steady state, single gas permeation measurements is depicted in Fig. 1, see also [7-11]. As the sketch shows, gas is introduced in the annulus, flows through the membrane due to the pressure difference ΔP , and leaves the cell at the end of the tube.

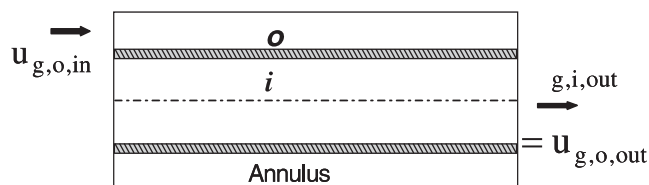


Fig. 1. Experimental set-up for the single gas permeation experiment

In this case, and for a homogeneous membrane, the general DGM equation [7-11] for species j in a mixture of N components is expressed by the relationship

$$\sum_{k=1, k \neq j}^N \frac{\tilde{x}_k \dot{n}_j - \tilde{x}_j \dot{n}_k}{D_{jk}^e} + \frac{\dot{n}_j}{D_{K,j}} = -\frac{P}{\tilde{R}T} \nabla \tilde{x}_j - \frac{\tilde{x}_j}{\tilde{R}T} \left(1 + \frac{B_0}{\eta_j D_{K,j}} \bar{P} \right) \nabla P \quad (1)$$

where $j = 1$ to N .

The driving forces are included in the right-hand part of eq. (1) in terms of total pressure and molar fraction (partial pressure) gradients, while the resulting fluxes, \dot{n}_j , appear at the left-hand side of the equation. For single gas permeation the DGM eq. (1) reduces to:

$$\dot{n}_j = -\frac{1}{\tilde{R}T} \left(\frac{4}{3} K_0 \sqrt{\frac{8\tilde{R}T}{\pi\tilde{M}_j}} + \frac{B_0}{\eta_j} \bar{P} \right) \nabla P. \quad (2)$$

For cylindrical coordinates and a relatively moderate membrane thickness the expression

$$\frac{\dot{N}_j}{\Delta P} = -\frac{2\pi L}{\tilde{R}T \ln\left(\frac{r_{m,o}}{r_{m,i}}\right)} \left(\frac{4}{3} K_0 \sqrt{\frac{8\tilde{R}T}{\pi\tilde{M}_j}} + \frac{B_0}{\eta_j} \bar{P} \right) \quad (3)$$

is obtained by integration of eq. (2).

With the additional assumption of tortuous, monodispersed capillaries, which are neither interconnected, nor change their cross-sectional area with their length, the three parameters of the dusty gas model can be expressed as

$$B_0 = F_0 \frac{d_p^2}{32}, \quad (4)$$

$$K_0 = F_0 \frac{d_p}{4} \quad (5)$$

$$F_0 = \frac{\varepsilon}{\tau}, \quad (6)$$

and are, thus, reduced to a set of only two morphological parameters, namely the diameter of the assumed capillaries

$$d_p = \frac{8B_0}{K_0}, \quad (7)$$

and

$$\frac{\varepsilon}{\tau} = \frac{(K_0)^2}{2B_0}, \quad (8)$$

In eq. (3), \bar{P} is the mean pressure in the membrane, $\bar{P} = (P_o + P_i)/2$, ΔP is the pressure drop, $\Delta P = P_o - P_i$. In experiments with a homogeneous membrane the pressure level, i.e. \bar{P} , is varied, while the pressure difference, ΔP , and P_i , P_o , or both are measured. Additionally, the gas flow rate, which permeates through the membrane, is determined, and converted to the gas molar flow rate, \dot{N}_j . With known geometry of the membrane (L , $r_{m,o}$, $r_{m,i}$) and gas properties, the parameters of the dusty gas model, K_0 and B_0 , can then be specified, compare also with [12]. Specifically, and due to the linearity of eq. (3), the Knudsen coefficient, K_0 , is derived from the intercept, and the permeability constant, B_0 , from the slope of a plot of the ratio $\dot{N}_j/\Delta P$ (termed as permeability coefficient) versus \bar{P} .

In case of any additional homogeneous layer on the original membrane, the described series of permeation experiments are repeated and eq. (3) can be applied to calculate the pressure at the interface between the first and the second layer of the composite. In this manner, pressures and flux are known for the second layer, so that the derivation of K_0 and B_0 can be specified also for this layer, in exactly the previously discussed way. Recursively, the parameters of every layer of any composite membrane can be derived individually, provided that all intermediate membranes, starting from the support and ending with the final composite, are available. The features of investigated membrane and results of this derivation are summarized in Tables 1 & 2.

Case A: $L = 150$ mm

$d_{m,o} = 10$ mm

$d_{m,i} = 7$ mm (approx.)

Table 1. Parameters of all membrane's layers for case A

Layer	Composition	Nom. pore diameter [m]	Thickness [m]	K_0 [m]	B_0 [m ²]	d_p [m]	$\frac{\varepsilon}{\tau}$
Support	$\alpha\text{-Al}_2\text{O}_3$	3.0×10^{-6}	1.5×10^{-3}	9.34×10^{-8}	3.58×10^{-14}	3.07×10^{-6}	0.122
1 st layer	$\alpha\text{-Al}_2\text{O}_3$	1.0×10^{-6}	25×10^{-6}	4.11×10^{-8}	9.47×10^{-15}	1.84×10^{-6}	0.089
2 nd layer	$\alpha\text{-Al}_2\text{O}_3$	0.2×10^{-6}	25×10^{-6}	9.40×10^{-9}	2.24×10^{-16}	0.19×10^{-6}	0.197
3 rd layer	$\alpha\text{-Al}_2\text{O}_3$	60×10^{-9}	25×10^{-6}	5.97×10^{-9}	5.69×10^{-17}	76×10^{-9}	0.313
4 th layer	$\gamma\text{-Al}_2\text{O}_3$	6.0×10^{-9}	2×10^{-6}	1.11×10^{-9}	2.18×10^{-18}	16×10^{-9}	0.283

Case B: $L = 150$ mm $d_{m,o} = 10$ mm $d_{m,i} = 7$ mm (approx.)**Table 2.** Parameters of all membrane's layers for case B

Layer	Composition	Nom. pore diameter [m]	Thickness [m]	K_0 [m]	B_0 [m ²]	d_p [m]	$\frac{\varepsilon}{\tau}$
Support	$\alpha\text{-Al}_2\text{O}_3$	3.0×10^{-6}	1.5×10^{-3}	9.34×10^{-8}	3.58×10^{-14}	3.07×10^{-6}	0.122
1 st layer	$\alpha\text{-Al}_2\text{O}_3$	1.0×10^{-6}	25×10^{-6}	4.11×10^{-8}	9.47×10^{-15}	1.84×10^{-6}	0.089
2 nd layer	$\alpha\text{-Al}_2\text{O}_3$	0.2×10^{-6}	25×10^{-6}	9.40×10^{-9}	2.24×10^{-16}	0.19×10^{-6}	0.197
3 rd layer	$\alpha\text{-Al}_2\text{O}_3$	60×10^{-9}	25×10^{-6}	5.97×10^{-9}	5.69×10^{-17}	76×10^{-9}	0.313
4 th layer	TiO ₂	5.0×10^{-9}	2×10^{-6}	9.17×10^{-10}	1.51×10^{-18}	13.2×10^{-9}	0.278

Though the identification of K_0 and B_0 can be done with only one gas at only one temperature, a large amount of experiments have been conducted in the present work for different gases at various temperatures.

Influence of top layer

The role of top layer (permselective layer) in an asymmetric membrane is to enhance the separation properties of the composite membrane. It should also be noticed that a composite membrane may exhibit asymmetry dependent fluxes due to non-isometric pressure profiles [9]. As the top layer thickness is very small (~ 2 μm) so it can not sustain alone the pressure differences required to achieve reasonable fluxes. Hence it is deposited on support/intermediate membrane layers to provide the required mechanical strength. A simulation analysis for three different gases was done to study the influence of temperature, flow direction and the top layer's material on the gas flow rates and pressure profiles in the composite membrane. Simulation study has been done for two cases which correspond to two different top layer materials. Two constant pressures (1 and 2 bar) on the two sides of the membrane and three different temperatures have been taken for the calculations. The membrane structural parameters used were identified by [11]. However, a shorter membrane length was considered in these simulations. Membrane structural parameters and the geometrical information for both cases are given in Tables 1 and 2. All parameters of the membrane layers are same in both cases excluding the parameters of the top layer (permselective layer). In case A, the top layer is made of $\gamma\text{-Al}_2\text{O}_3$ while in case B, the top layer is made of TiO₂.

The simulations have been completed using the dusty gas model equation eq. (3) for the permeation of three different gases (H_2 , N_2 , SF_6) at three different temperatures (20 °C, 100 °C, 200 °C) for both types of composite membrane (case A & Case B). The influence of flow direction was quantified by alternatively setting two different pressures on the membrane sides (differentiating

that the gas first enters the membrane support or the permselective layer). Simulation results are presented in Figs 2 and 3.

Figure 2 shows for the calculated values of the ratio of molar flow rate to pressure drop (permeability coefficient) plotted against the temperature for Case A for all gases. It can be seen that the ratio of molar flow rate to pressure drop decreases as the molar mass of the gas increases. The ratio of molar flow rate to pressure drop decreases also by increasing the temperature, as the gas viscosity increases by the temperature. The major effect to show in these figures is the influence of flow direction on the ratio of molar flow rate to pressure drop (permeability coefficient). In both figures, full lines correspond to the gas entering first the support membrane and the broken lines correspond to the gas entering first the permselective layer. It can be seen that in both cases (A & B), the ratio of molar flow rate to pressure drop is higher when the gas first enters the support membrane.

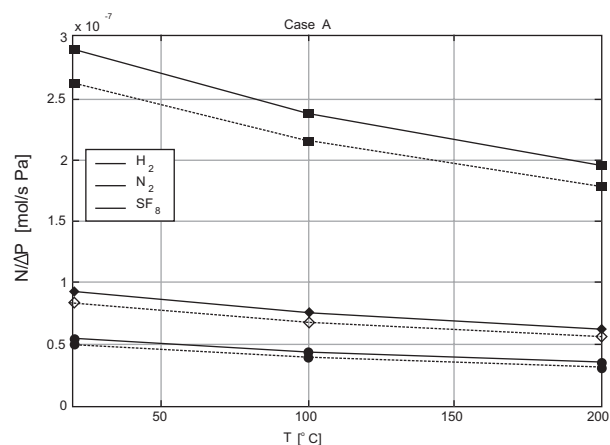


Fig. 2. Ratio of molar flow rate to pressure drop versus temperature for three different gases (solid lines: gas entering first the support layer, broken lines: gas entering first the permselective layer)

This behaviour of the composite membrane can be attributed to the local distribution of resistances in the membrane [9-10]. The differences in ratios of molar flow rate to pressure drop (permeability coefficients) are upto 9% for case A and about 8% for the case B (Fig. 3).

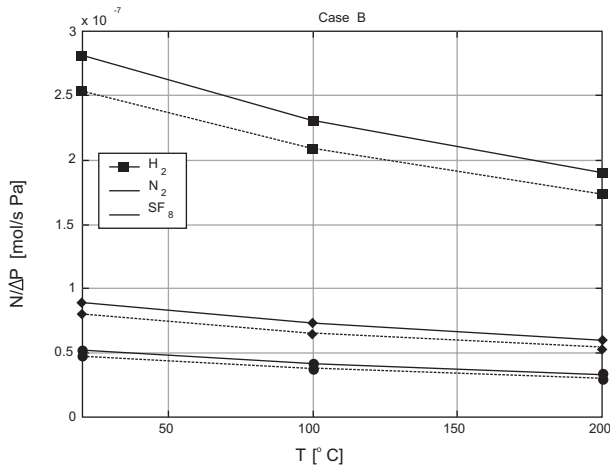


Fig. 3. As in Fig. 2, however for case B membrane

This deviation can be critical when employing the porous membrane for selective dosing of educts [13-14]. If both diagrams are compared, it can be further seen that the ratio of molar flow rate to pressure drop is higher in Case A and Case B. This is due to the fact that the permselective layer made of TiO_2 (case B) has smaller pores than the permselective layer made of $\gamma\text{-Al}_2\text{O}_3$ (case A). It is also to notice here that the rise in molar mass of the gas reduces the above mentioned deviation in both cases.

Figures 4 to 7 show the calculated pressure profiles in all membrane layers for different temperatures and gases. Again, the analysis has been done for two alternative situations, gas entering the support membrane first and gas entering the permselective layer first. In all figures, zero corresponds to support side of the membrane while 5 corresponds to the permselective side of the composite membrane and 1 to 4 are the interfaces of intermediate layers in the composite membrane. Consequently, the full lines correspond to the pressure profiles when gas enters the support layer first and broken lines correspond to the pressure profiles when gas enters the permselective layer first.

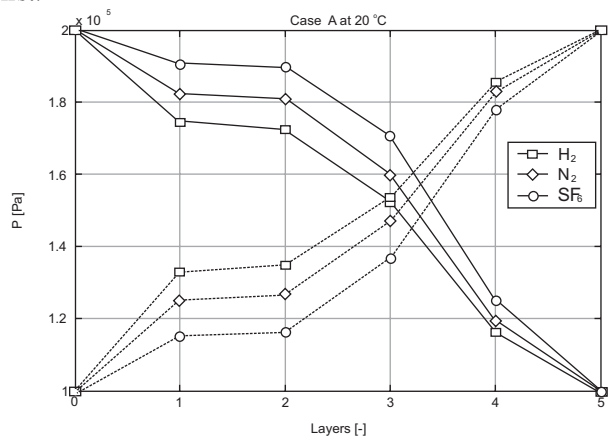


Fig. 4. Pressure profiles in the composite membrane at 20°C for three different gases at the pressure level of 1 & 2 bars.

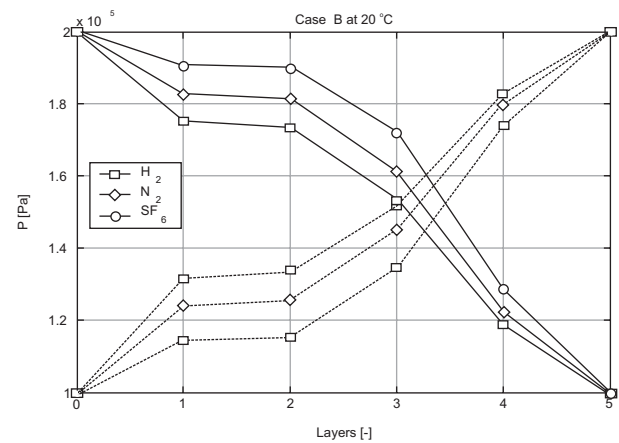


Fig. 5. Fig. 4. Pressure profiles in the composite membrane at 20°C for three different gases at the pressure level of 1 & 2 bars

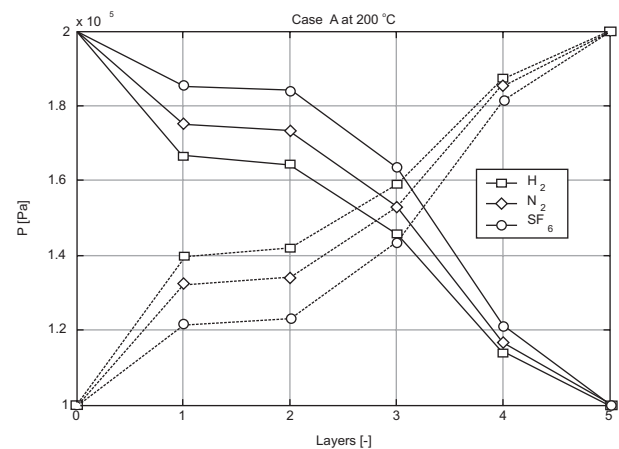


Fig. 6. Pressure profiles in the composite membrane at 200°C for three different gases at the pressure level of 1 & 2 bars

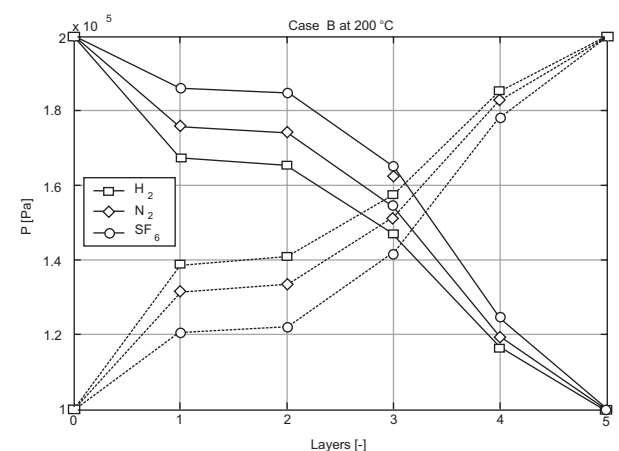


Fig. 7. As Fig. 6, though for case B membrane

In a catalytic membrane reactor, pressure effects can contribute to a better accessibility of reactants to catalyst, which can improve the conversion rate in some reactions [15]. The analysis of pressure profiles shown in Figs 4 to 7 reveals that the pressure drop in case B (TiO_2 layer as a permselective layer), for all gases and temperatures, is

comparatively higher than in case A ($\gamma\text{-Al}_2\text{O}_3$ as a permselective layer). The permselective layer influences the local distribution of pressure drop in every individual layer of the composite membrane. In spite of this, the pressure drop is higher in the 3rd layer of the membrane for all gases and temperatures in both cases. Moreover, it has been found in the analysis that the pressure drop in the permselective layer rises as the molar mass of the gas increases.

Conclusion

The single gas permeation experiments have been carried out for every membrane layer. In this way, the identification of mass transfer parameters could be conducted separately for every individual layer of the composite. Doing so, the influences of temperature, pressure and molar mass of the gas can be precisely understood and accurately predicted by means of the dusty gas model, which successfully combines the mechanisms of Knudsen diffusion, viscous flow and molecular diffusion. The simulation analysis shows the influence of flow direction and top layer on the mass transfer through the membrane. The analysis reveals that the choice of flow direction may be significant, especially when employing the membrane for the selective dosing of educts in a catalytic reactor. It has also been shown that the fluxes may depend on the flow direction in a composite membrane. Also the choice of the material of permselective layer is substantial in terms of pressure drop and fluxes. It is evident from the simulation analysis that different permselective layers can considerably shift the pressure profile in the composite membrane.

Acknowledgement

The financial support of the German Research Foundation (Research group "Membrane supported reaction Engineering", FOR 447/1-1) is gratefully acknowledged.

REFERENCES

1. J. M. S. Henis and M. K. Tripodi, "Composite membranes for gas separation: The resistance model approach", *Journal of Membrane Science*, Vol. 8, 1981, pp. 233-246.
2. A. Fouda, Y. Chen, J. Bai and T. Matsuura, "Wheatstone bridge model for the laminated polydimethylsiloxane/ polyethersulfone membrane for gas separation", *Journal of Membrane Science*, Vol. 64, 1991, pp. 263-271.
3. M. Mulder, *Basic Principles of Membrane Technology*, Boston: Kluwer Academic Press, 1991.
4. J. Coronas and J. Santamaria, "Catalytic reactors based on porous membranes", *Catalysis Today*, Vol. 51, 1999, pp. 377-389.
5. P. Drechsel, J. L. Hoard and F.A. Long, "Diffusion of acetone into cellulose nitrate films and study of the accompanying orientation", *Journal of Polymer Science*, Vol. 10, 1953, pp. 241-252.
6. A. E. Polotsky and G. A. Polotskaya, "Study on the top layer structure of the composite membranes", *Journal of Membrane Science*, Vol. 140, 1998, pp. 97-102.
7. A. Tuchlenski, P. Uchytel and A. Seidel-Morgenstern, "An experimental study of combined gas phase and surface diffusion in porous glass", *Journal of Membrane Science*, Vol. 140, No. 2, 1998, pp. 165-184.
8. S. Thomas, R. Schäfer, J. Caro and A. Seidel-Morgenstern, "Investigation of mass transfer through inorganic membranes with several layers", *Catalysis Today*, Vol. 67, No. 1-3, 2001, pp. 205-216.
9. S. Thomas and Kontrollierte Eduktzufuhr, "Membranreaktoren zur Optimierung der Ausbeute gewünschter Produkte in Parallel- und Folgereaktionen", PhD thesis, Otto-von-Guericke-Universität, Magdeburg, Germany, 2003.
10. P. Capek and A. Seidel-Morgenstern, "Multicomponent mass transport in porous solids and estimation of transport parameters", *Applied Catalysis A: General*, Vol. 211, No. 2, 2001, pp. 227-237.
11. P. Uchytel, O. Schramm and A. Seidel-Morgenstern, "Influence of the transport direction on gas permeation in two-layer ceramic membranes", *Journal of Membrane Science*, Vol. 170, No. 2, 2000, 215-224.
12. C. Fernández-Pineda, M. A. Izquierdo-Gil and M. C. García Payo, "Gas permeation and direct contact membrane distillation experiments and their analysis using different models", *Journal of Membrane Science*, Vol. 198, No. 1, 2002, pp. 33-49.
13. U. Beuscher and C.H. Gooding, "The influence of the porous support layer of composite membranes on the separation of binary gas mixtures", *Journal of Membrane Science*, Vol. 152, No. 1, 1999, pp. 99-116.
14. A. Tuchlenski, O. Schramm and A. Seidel-Morgenstern, "Steady state and dynamic mass transfer of gases in porous materials", *Collection of Czechoslovak Chemical Communications*, Vol. 62, No. 7, 1997, pp. 1043-1056.
15. E. E. Iojoiu, J. C. Walmsley, H. Raeder, S. Miachon and J. A. Dalmon, "Catalytic membrane structure influence on the pressure effects in an interfacial contactor catalytic membrane reactor applied to wet air oxidation", *Catalysis Today*, Vol. 104, No. 2-4, 2005, pp. 329-335.

Nomenclature

B_0	m^2	Permeability constant in dusty gas model
d	m	Diameter
D	$m^2 s^{-1}$	Diffusion coefficient
F_0	-	Ratio of effective to molecular diffusion coefficient
K_0	m	Knudsen coefficient in dusty gas model
L	m	Length
\tilde{M}	$kg\ mol^{-1}$	Molar mass
\dot{n}	$mol\ m^{-2} s^{-1}$	Molar flux
\dot{N}	$mol\ s^{-1}$	Molar flow rate
P	Pa	Pressure
\bar{r}	m	Mean membrane radius
\tilde{R}	$J\ mol^{-1} K^{-1}$	Universal gas constant
\tilde{x}	-	Mole fraction

Indices

e	Effective
j,k	Species in the mixture
K	Knudsen
m	Membrane
o	Outer, annulus side
p	Pore

Greek symbols

ε	-	Porosity
η	$Pa\ s^{-1}$	Viscosity
τ	-	Tortuosity